Macromolecular Research, Vol. 10, No. 6, pp 325-331 (2002)

Phase Behavior of a PEO-PPO-PEO Triblock Copolymer in Aqueous Solutions: Two Gelation Mechanisms

Moon Jeong Park and Kookheon Char*

School of Chemical Engineering & Institute of Chemical Processes, Seoul National University, Seoul 151-744, Korea

Hong Doo Kim

Department of Chemistry, Kyunghee University, Yongin 449-701, Korea

Chang-Hee Lee, Baek-Seok Seong, and Young-Soo Han

Korea Atomic Energy Research Institute, Yusong, Daejon 305-600, Korea

Received Sept. 6, 2002; Revised Nov. 7, 2002

Abstract: Phase behavior of a PEO-PPO-PEO (Pluronic P103) triblock copolymer in water is investigated using small-angle neutron scattering (SANS), small-angle X-ray scattering (SAXS), dynamic light scattering (DLS) and rheology. Pluronic P103 shows apparent two gel states in different temperature regions. The first sol-to-gel transition at a lower temperature (*i.e.*, the hard gel I state) turns out to be the hexagonal microphase as evidenced by the combined SANS and SAXS and the frequency dependence of both G' and G'' in rheology. In contrast to the hard gel I, the second sol-to-gel transition (*i.e.*, the hard gel II state) at a higher temperature represents the block copolymer micelles in somewhat disordered state rather than the ordered state seen in the hard gel I. Moreover, turbidity change depending only on the temperature with four distinct regions is observed and the large aggregates with size larger than 5,000 nm are detected with DLS in the turbid solution region. Based upon the present study, two different gelation mechanisms for aqueous PEO-PPO-PEO triblock copolymer solutions are proposed.

Keywords: gelation mechanisms, PEO-PPO-PEO triblock copolymer, turbidity, hydrophobic interaction.

Introduction

Block copolymers containing both a hydrophilic block such as poly(ethylene oxide) (PEO) and a hydrophobic block such as poly(propylene oxide) (PPO) or poly(butylene oxide) (PBO) connected by a covalent bond in a chain generally form micelles in a selective solvent due to the self-assembling nature of amphiphilic chains.[1-5] Aqueous solutions of this kind of amphiphilic block copolymers at high concentrations typically undergo the sol-to-gel transition with increase in temperature. It is well known that for Pluronic F127 with a nominal composition $EO_{99}PO_{65}EO_{99}$, the average number of unimers per micelle (*i.e.*, aggregation number) increases with increase in solution temperature and concentration because the unimer-micelle equilibrium is further shifted toward the micellar state. When the aggregation number reaches the plateau value, the micelles eventually come in contact with one another and these contacts cause entanglements among hydrophilic corona PEO chains.[6] It was reported that the cubic structure is formed by the spherical micelles confirmed with small-angle neutron scattering (SANS) when the volume fraction occupied by the micelles reaches a critical value of 0.53.[9-12]

However, when the molecular weight of PEO chains is far below the entanglement molecular weight (M_e) of 1,600,[13,14] the solution behavior is expected to be quite different from the Pluronic F127 since the micelles cannot pack through the entanglement of PEO corona chains. For instance, Pluronic P94 with a nominal composition $EO_{21}PO_{47}EO_{21}$ containing shorter EO blocks has been shown to have two-gel like structure (*i.e.*, a hard gel state at a lower temperature and a soft gel state at a higher temperature).[4, 15-17] We noted, however, that many previous studies have mainly focused on the gelation mechanism of the lower hard gel state, namely the gelation through micellar packing, and the gelation behavior and the mechanism of gel formation at a higher temperature have yet not been addressed in detail.

Most recently, we reported a study on the micellar ordering in gels formed by a low molecular weight triblock copoly-

*e-mail : khchar@plaza.snu.ac.kr

mer.[18] We proposed different gelation mechanisms of the two gel states formed by a Pluronic P103 ($EO_{17}PO_{60}EO_{17}$) containing longer PO block, which is comparable to the F127, but with shorter EO blocks since the P103 apparently shows two hard gel states in two different temperature regions.

The results presented here complement earlier studies and reinforce the conclusion on the gelation mechanism based on the phase diagram of the Pluronic P103 and the turbidity change as a function of temperature. The size distribution of the Pluronic P103 in water is observed using DLS and SANS, SAXS and rheology measurement are employed to investigate the structural change of micelles with increase in temperature. Based on these results, we discuss the difference between the first gelation at a low temperature and the second gelation at a high temperature. Furthermore, we would like to generalize different gelation mechanisms on aqueous solutions of Pluronics containing short hydrophilic PEO end blocks.

Experimental

Materials. A commercial grade of Pluronic P103 with a nominal composition $EO_{17}PO_{60}EO_{17}$ was kindly donated by BASF and used without further purification. The nominal molecular weight of this copolymer is 4,950 and the weight fraction of PEO in the triblock copolymer is approximately 30%. An aqueous solutions of Pluronic P103 prepared with different polymer concentration (in units of wt%) were heated to 90 °C for 10 min and gently agitated in sealed vials. Those solutions were then stored below 5 °C for more than 1 day.

Phase Diagram. Vials of 4 mL were used for the tube inversion method to construct the phase diagram and the vials sealed with Teflon tape were placed in a water bath which can control temperature with an accuracy of ± 0.01 °C. To ensure equilibrium, more than 20 min of equilibration time was allowed for each temperature and measurements were made every 0.5 °C from 1 to 90 °C. A change from a mobile state to an immobile one was determined by inverting the vial. *Hard gels* were defined as no movement of a liquid meniscus in a vial for more than 5 min upon inversion of the vial while *soft gels* were defined as any detection of slow movement of the meniscus over a period of 5 min. *Sols* were defined as a state in which the solution readily flows to the bottom of the vial within 1 min upon inversion.

Turbidity Measurement. A light scattering set-up was used to detect the turbidity of aqueous solutions of the Pluronic P103 as a function of temperature. Temperature scan was carried out at a heating rate of 0.5 °C/min. Measurements were made in transmission mode and transmitted light intensity was monitored with a photomultiplier tube (PMT). A homemade light scattering apparatus is equipped with a He-Ne laser with wavelength $\lambda = 632.8$ nm. All the solutions for the turbidity measurement were filtered with filters of 0.45 μm pore size to avoid any effect of impurity on the turbidity.

Dynamic Light Scattering (DLS). Dynamic light scattering measurements were made at a 90° scattering angle with respect to the incident light path to a liquid sample holder using a Brookhaven DLS (BI-9000AT) equipped with a digital autocorrelator and a photon counter. A light source of a He-Ne laser with $\lambda = 632.8$ nm was used. Information on the size distribution of micelles and/or clusters was obtained by the inverse Laplace transformation of scattering data using the CONTIN program. All the measurements were taken after 30 min of equilibration time and all the solutions were filtered using 0.45 μm pore size filters to avoid the effect of impurity.

Small-Angle Neutron Scattering (SANS). Small-angle neutron scattering experiments were performed using an 8 m SANS facility at the Korea Atomic Energy Research Institute (KAERI) equipped with a two-dimensional position-sensitive detector. The sample-to-detector distance of 4.61 m and the neutron wavelength of 5.08 Å was used to yield scattering vectors $q = (4\pi/\lambda)\sin(\theta/2)$ in the range of $0.07 \sim 1.0\ nm^{-1}$ and the neutron beam has a wavelength resolution ($\Delta\lambda/\lambda$) of 10%. A beam stopper with a diameter of 55 mm was placed in front of the detector to prevent the damage of the detector center from direct neutron beam. For the temperature control, a circulating bath in the range of 0 to 100 °C with an accuracy of ± 0.01 °C was employed.

Deuterium oxide (D_2O, 99.9 atom% D) purchased from Aldrich Chemical was used to obtain good contrast and low background for the neutron scattering experiments. The copolymer was dissolved at room temperature with 100% D_2O and samples were placed between two sealed quartz windows with a flight path of 2 mm after filtering the samples with filters of 0.45 μm pore size. All the measurements were taken after 30 min of equilibration time and all the scattering data obtained were corrected for sample transmission, incident wavelength distribution, and background originating from the quartz cells filled with D_2O. The resulting one-dimensional scattering data calibrated with a well-characterized silica standard consist of the differential scattering cross-section, dS/dW, as a function of q in absolute units of cm^{-1}.

Small-Angle X-ray Scattering (SAXS). Synchrotron SAXS measurements were carried out at the 4C1 SAXS beamline in Pohang Light Source (PLS) consisting of 2 GeV LINAC accelerator, Si (111) double crystal monochromators, ion chambers, and a two-dimensional position sensitive detector with 1242 × 1152 pixels. The wavelength (λ) of the synchrotron beam was 1.609 Å and the energy resolution ($\Delta\lambda/\lambda$) was 5×10^{-4}. Typical beam size was smaller than $1 \times 1\ mm^2$ and the sample-to-detector distance was 93 cm. Scattering profiles were obtained as a function of temperature and the data were then corrected for absorption, air and imide film scattering. To ensure equilibrium, more than 30 min of equilibration time was allowed.

Rheology. Rheometer RMS-800 (Rheometrics) in a conicylinder geometry (cup diameter, 52 mm; bob diameter, 50 mm; bob length, 20 mm; and bottom gap, 0.2 mm) was used to measure dynamic viscoelastic storage modulus (G'), loss modulus (G''), and complex viscosity (η^*) of the solutions as a function of temperature. Temperature scans at a fixed frequency of 0.5 rad/s were carried out at a heating rate of 0.5 °C/min. Strain was fixed at 2.7%, which was small enough to ensure linear viscoelasticity.[19]

Results and Discussion

Phase Diagram: Two Different Gel States and Turbidity Change. The phase diagram of a PEO-PPO-PEO (Pluronic P103) triblock copolymer in water, measured with the tube inversion method, is shown in Figure 1(a). At a lower temperature, hard gel I is formed only at concentrations above 29 wt% and degelation was also observed with increase in temperature. When the solution temperature is increased up to a 43 °C, all solutions become turbid independent of the concentration. Upon further heating, another hard gel phase called the hard gel II is observed in the concentration range from 14 to 32 wt%. For copolymer concentrations ranging from 12 to 32 wt%, soft gels are also observed around the hard gel II boundary in the temperature region from about 40 to 70 °C. The cloud zone is believed to the coexistence state of a hard gel I and a turbid soft gel due to the phase mixing.[18]

We also note that aqueous solutions of the Pluronic P103 show turbidity change depending only on the temperature not on the polymer concentration. As presented in Figure 1(b), the temperature range of an aqueous solution can be classified into four distinct regions. In region I, the solution is transparent up to about 30 °C. In region II, turbidity increases with increase in temperature and in region III turbidity decreases upon further heating. The aqueous solutions of the Pluronic P103 show the maximum turbidity at around 54 °C. In region IV, the turbidity remains almost constant before the copolymers eventually precipitate out of water at about 86 °C. As we have already mentioned, for the concentration above 29 wt% with the first hard gel I phase, there also exists the cloud zone between the region I and region II.

Dynamic Light Scattering: Change of Size Distribution of Micelles, Clusters, and Large Aggregates with Increase in Temperature. Figure 2 shows the DLS measurements of a 29 wt% Pluronic P103 in water undergoing two sol-to-gel transitions. The size of unimers is known to be around 1~2 nm and the micelles are around 10~50 nm while micelle clusters can vary in size anywhere above 100 nm. At a temperature of 25 °C in the hard gel I, the micellar motion is clearly dominant. This implies that the hard gel I is formed by the micelle packing. At a temperature of 32 °C in the cloud zone, the motion of micellar or even larger clusters

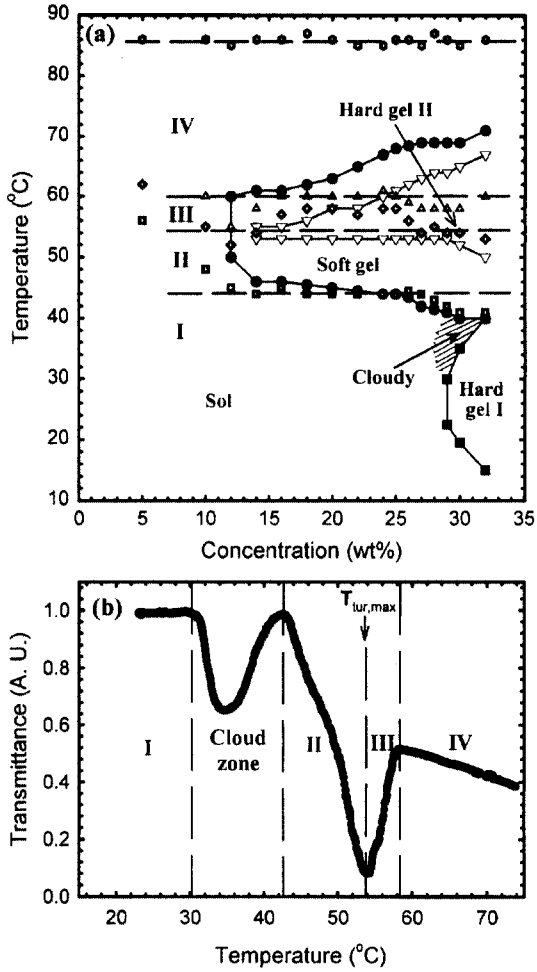

Figure 1. (a) Phase diagram and turbidity measurement of Pluronic P103 in water determined by the tube inversion method: (■) hard gel I boundary, (▽) hard gel II boundary, (●) soft gel boundary(ref. 18). (b) Relative transmittance of a 29 wt% aqueous solution of Pluronic P103 as a function of temperature: ~■, (I) up to 30 °C, minimal turbidity region; (cloud zone) 30 to 42.5 °C, two-phase region; ■~◆, (II) 42.5 to 54 °C, turbidity-increase region; ◆~▲, (III) 54 to 58.5 °C, turbidity-decrease region; ▲~●, (IV) 58.5 to 86 °C, constant turbidity region just before the global chain collapse (ref. 18).

with size larger than 5,000 nm as well as the micellar motion is detected. However, no large clusters at this temperature were observed for a concentration of 24 wt%, which is transparent (data not shown). At a temperature of 43 °C in the region II representing the turbidity-increase, two modes of both the micellar motion and the motion of large clusters are observed. At temperatures of 55 °C in the region III representing the turbidity-decrease and of 65 °C in the region IV showing the constant turbidity, only the motion of large clusters is detected for all the concentrations examined.

This implies that large aggregates of micelles are formed due to the temperature-induced hydrophobic attraction. The

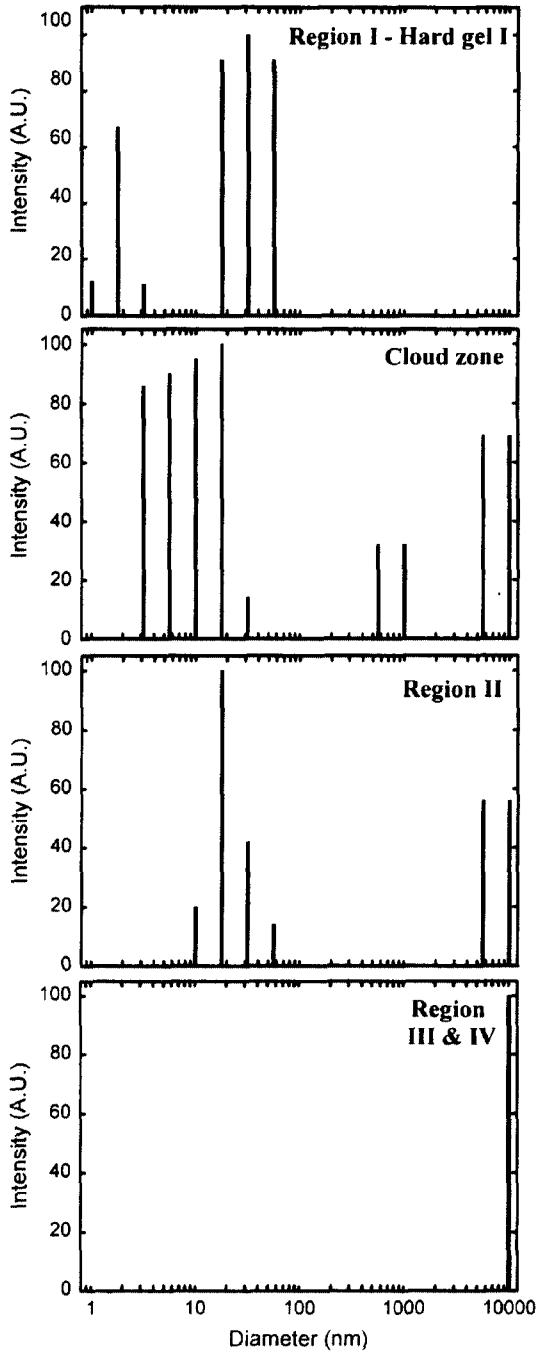

Figure 2. Size distribution of unimers, micelles, and micelle clusters for a 29 wt% aqueous solution of Pluronic P103 measured with dynamic light scattering: region I-hard gel I (25 °C), cloud zone (32 °C), region II (43 °C), regions III & IV (55 & 65 °C). Size detection limit is about 10,000 nm.

formation of these large aggregates of micelles with size above microns has recently been reported with another Pluronic L64 ($EO_{13}PO_{30}EO_{13}$) based on the ultrasonic relaxation studies.[21] This report supports our DLS results and we believe that the formation of large aggregates is the general

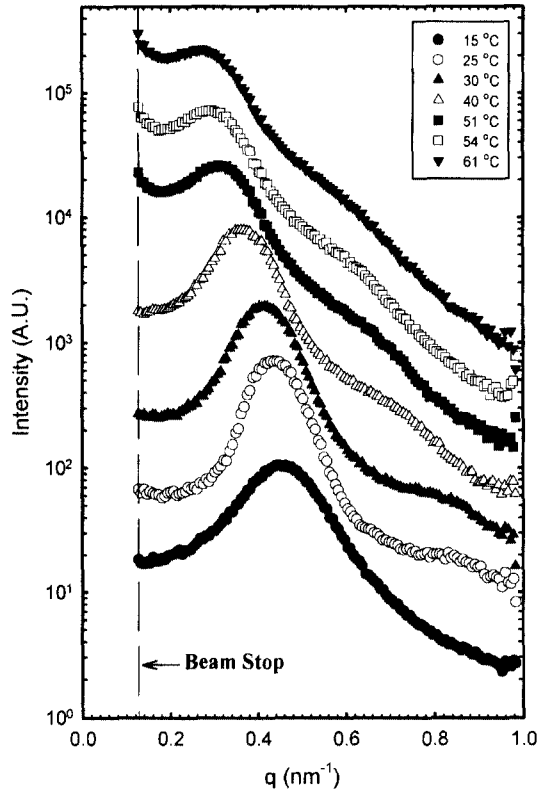

Figure 3. SANS profiles of a 29 wt% aqueous solution of Pluronic P103 upon heating. Each data set was vertically shifted for clarity. Temperatures of the block copolymer solution are indicated in the figure.

behavior of Pluronic series containing relatively short PEO end blocks since the short PEO chains do not act as strong steric layers. It is also interesting to note here that for aqueous solutions of Pluronic P103, the size distribution among unimers, micelles, and micellar clusters is quite temperature-sensitive and closely related with turbidity rather than the apparent sol or gel state.

Small-Angle Neutron Scattering: Structural Change with Increase in Temperature. SANS measurements were made at various temperatures in order to obtain information on the structural change during the sol-to-gel transitions. In Figure 3, results for a 29 wt% aqueous solution of the Pluronic P103 are shown in a semilogarithmic plot of scattered intensity as a function of scattering vector q. Each data set was vertically shifted for clarity and it should be noted here that in the present work we focused only on the high concentration region undergoing the sol-to-gel transitions. At a temperature of 15 °C corresponding to the sol state, only the first peak is observed indicating no long-range interactions among the micelles, since the unimer-micelle equilibrium is not totally shifted toward the micellar state due to the fact that the PPO middle block is less hydrophobic at low temperature. While at a temperature of 25 °C in the hard gel I

region, the second hump as well as the narrow first peak is observed. We believe that the first peak is equivalent to the micellar d-spacing at about 14.2 nm and the second hump represents the ordered structure. At a temperature of 40 °C in the region I, the second hump as well as the first peak is shifted to lower q values. With increase in temperature up to 51 °C in the region II (*i.e.*, soft gel), the shape of scattering curve changes quite differently from that measured at lower temperatures. In other words, both the first peak and the second hump are further shifted to lower q values and those peaks are significantly broadened due to the fact that the microstructure is considerably changed between 40 and 51 °C. Such scattering profiles persist up to the region III and IV (*i.e.*, hard gel II). This implies that the microstructure of the hard gel II possibly driven by the macroscopic liquid-liquid phase separation owing to the attractive hydrophobic interaction among the PPO blocks is quite different from the microstructure of the hard gel I.

Small-Angle X-ray Scattering: Structure of Hard Gel I. To define the structure of gel states more clearly, synchrotron SAXS measurements were performed since the wavelength resolution of SAXS ($\Delta\lambda/\lambda = 5\times 10^{-4}$) was much smaller than that of SANS ($\Delta\lambda/\lambda = 10^{-1}$). Information on the equilibrium microdomain morphology of block copolymers can be obtained from the relative positions of these multiple peaks, since they exhibit different arrays depending on the shape of microdomain structure. As shown in Figure 4(a), the 2D SAXS pattern and the circular averaged 1D SAXS profile for a 29 wt% aqueous solution at a temperature of 25 °C corresponding to the hard gel I state showed the hexagonal phase as characterized by the ratio between positions of the first three diffraction rings of 1: $(3)^{1/2}$: $(4)^{1/2}$. This SAXS result is in excellent agreement with the frequency dependence of G' and G''. As shown in Figure 4(b), it indicates the typical frequency dependence of the hexagonal microphase since it is well known that the BCC spherical structure behaves as a solid, with the dynamic elastic shear modulus G' independent of frequency in the linear regime at high frequency while both G' and G'' for lamellar and hexagonal microphases are strongly frequency dependent for all the frequencies covered here.[21] Moreover, SAXS measurements were carried out with increase in temperature, and we did not obtain any information on the perfect ordered structure at higher temperature since the hard gel II state appears as a macroscopic gel or somewhat in a disrupted micellar state (data not shown).

Rheology: Effect of Concentration and Temperature. Figure 5(a) shows the change of G', G'', and η^* as a function of temperature for a 29 wt% Pluronic P103 in water, undergoing the two sol-to-gel transitions. In region I, the G' value changes abruptly at about 21 °C and the maximum G' value ($> 10^3$ Pa) is observed at around 25 °C corresponding to the hard gel I state. The temperature of the abrupt change in G' at around 21 °C is in excellent agreement with the sol-to-hard

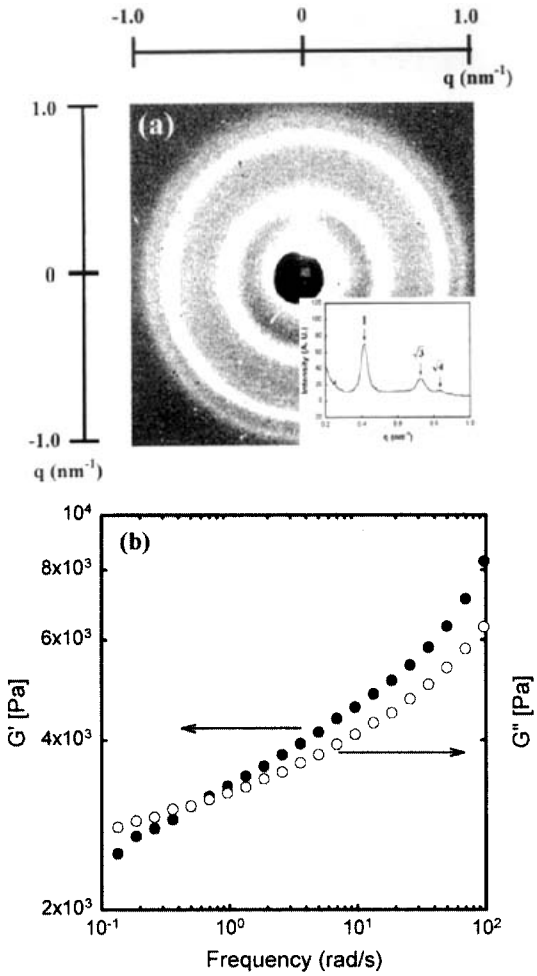

Figure 4. (a) 2D SAXS pattern and circular averaged 1D SAXS profile of a 29 wt% aqueous solution of Pluronic P103 at 25 °C corresponding the hard gel I state. A relative ratio between the positions of the first three diffraction rings of 1: $(3)^{1/2}$: $(4)^{1/2}$ demonstrates the hexagonally packed micelle structure. (b) Change of storage modulus (G') and loss modulus (G'') as a function of frequency for a 29 wt% aqueous solution of Pluronic P103 at 25 °C corresponding the hard gel I state.

gel transition temperature in the phase diagram. After degelation, G', G'', and η^* values do not significantly change upon heating up to the maximum turbidity temperature except a subtle change at the boundary between the cloud zone and the region II. However, the G' value again increases from the temperature at the maximum turbidity and the G' local maximum corresponds to the appearance of the hard gel II in the phase diagram. In other words, the aqueous Pluronic P103 solution with 29 wt% shows the apparent two maximum G' values indicating both the hard gel I and the hard gel II.

We also investigated the change of G' for various block copolymer concentrations. As shown in Figure 5(b), the

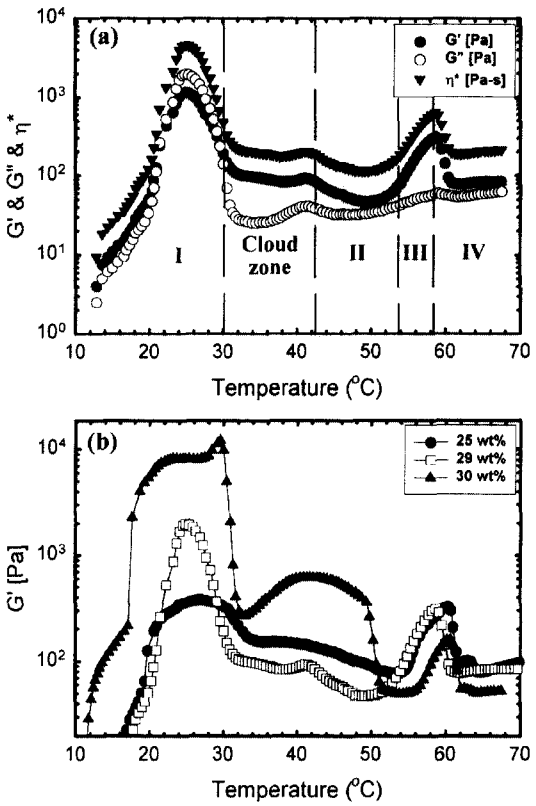

Figure 5. (a) Change of storage modulus (G'), loss modulus (G''), and complex viscosity (η^*) as a function of temperature for a 29 wt% aqueous solution of Pluronic P103. (b) Change of storage modulus (G') as a function of temperature for aqueous solutions of Pluronic P103 with different concentrations. Block copolymer concentrations are indicated in the figure(ref. 18).

absolute G' values and the behavior of the G' change at the first maximum are considerably concentration dependent. For a 25 wt% aqueous solution, the G' value does not discontinuously change at the first maximum temperature and the absolute G' value is also relatively small since the first sol-to-gel transition does not occur presumably due to the insufficient micelle packing density. However, at a concentration of 29 wt% undergoing the first sol-to-gel transition, the G' value is six times higher than the value for the 25 wt% solution and there is also an abrupt change in G' at the transition. As the solution concentration is increased up to 30 wt%, even higher value of G' ($> 10^4$ Pa) is observed and there exists a plateau G' in the temperature range between 20 and 30 °C. This implies that the first maximum G' is significantly dependent on the concentration indicating the degree of micellar packing density. In contrast, the behavior of the second maximum G' (*i.e.*, the local maximum value) at around 60 °C is almost independent of the concentration. Moreover recently, we reported that the hard gel II state could not be detected during cooling scan regardless of concentration.[18] This implies that the second gel phase driven by the macroscopic liquid-liquid phase separation is not easily rehydrated upon cooling and not thermoreversible. We believe that the large aggregates consisting of loosely bound micelles transform into more compact structure upon heating since the PEO endblocks become more hydrophobic and partially dehydrated resulting in the phase mixing with PPO and at the same time, the hydrophobic attraction between the PPO cores is even more reinforced. Upon further heating, water finally acts as a poor solvent for both PEO and PPO chains and this induces a state just before the global chain collapse in water (*i.e.*, regions III and IV).

Conclusions

The gelation behavior of aqueous solutions of a PEO-PPO-PEO (Pluronic P103) is investigated. We note that two gel states are formed by two different gel mechanisms and the turbidity change depending only on temperature with four distinct regions is observed with increase in temperature. Large aggregates or micelle clusters with size larger than 5,000 nm are detected with DLS in the turbid solution region and the fraction of large aggregates appears to increase with increase in temperature. The second hump representing the ordered long-range structure as well as the first peak equivalent to the micellar d-spacing is observed using SANS. To monitor the gel structure, SAXS experiments with better wavelength resolution were employed and the frequency dependence of G' and G'' in rheology was also observed. From those results, the hard gel I is believed to be due to the micellar packing in the hexagonal phase while the hard gel II is a macroscopic gel in a rather disrupted state. Rheological measurements show that the Pluronic P103 shows the apparent two maximum G' values indicating two sol-to-gel transitions and the G' behavior around the second maximum G' temperature does not significantly depend on the concentration. This leads us to conclude that for Pluronics having relatively short hydrophilic end blocks such as Pluronic P103, the macroscopic liquid-liquid phase separation driven by the attractive hydrophobic interaction between the hydrophobic PPO core phases upon heating cause the turbidity change and the second gelation at a higher temperature. We believe that the gelation at the lower temperature is related to the micellar growth and packing, while the gelation at the higher temperature involves the breakup of the micelle structure because the PEO chains become less hydrophilic and partially dehydrated resulting in the phase mixing with the PPO core phases upon heating.

Acknowledgement. We are very grateful to the financial support from the National Research Laboratory Fund (Grant M1-0104-00-0191) by the *Ministry of Science and Technology of Korea*, the Brain Korea 21 Program endorsed by the *Ministry of Education of Korea*, and the *Seoul National University Nanoelectronics Institute*. Experiments performed at

Korea Atomic Energy Research Institute (KAERI) and Pohang Light Source (PLS) were supported by MOST.

References

(1) M. Malmsten and B. Lindman, *Macromolecules*, **25**, 5440 (1992).
(2) O. Glatter, G. Scherf, K. Schill, and W. Brown, *Macromolecules*, **27**, 6046 (1994).
(3) P. Alexandridis, J. F. Holzwarth, and T. A. Hatton, *Macromolecules*, **27**, 2414 (1994).
(4) P. Bahadur and K. Pandya, *Langmuir*, **8**, 2666 (1992).
(5) G. E. Yu, Y. Deng, S. Dalton, Q. G. Wang, D. Attwood, C. Price, and C. Booth, *J. Chem. Soc. Faraday Trans.*, **88**, 2537 (1992).
(6) A. V. Kabanov, I. R. Nazarova, I. V. Astafieva, E. V. Batrakova, V. Y. Alakhov, A. A. Yaroslavov, and V. A. Kobanov, *Macromolecules*, **28**, 2303 (1995).
(7) S. Miyazaki, Y. Ohkawa, M. Takada, and D. Attwood, *Chem. Pharm. Bull.*, **40** (8), 2224 (1992).
(8) R. Bhardwaj and J. Blanchard, *J. Pharm. Sci.*, **85** (9), 915 (1996).
(9) K. Mortensen, W. Brown, and B. Norden, *Phys. Rev. Lett.*, **68**, 2340 (1992).
(10) K. Mortensen and J. S. Pedersen, *Macromolecules*, **26**, 805 (1993).
(11) G. Wanaka, H. Hoffmann, and W. Ulbricht, *Colloid Polym. Sci.*, **268**, 101 (1990).
(12) I. Goldmints, F. K. Gottberg, K. A. Smith, and T. A. Hatton, *Langmuir*, **13**, 3659 (1997).
(13) A. M. G. Dasilva, E. J. M. Filipe, J. M. R. Doliveira, and J. M. G. Martinho, *Langmuir*, **12**, 6547 (1996).
(14) J. D. Ferry, in *Viscoelastic Properties of Polymers*, 3rd Ed., New York, 1989.
(15) Y. Liu, S.-H. Chen, and J. S. Huang, *Macromolecules*, **31**, 2236 (1998).
(16) S. Hvidt, E. B. Jørgensen, W. Brown, and K. Schillén, *J. Phys. Chem.*, **98**, 12320 (1994).
(17) E. B. Jørgensen, S. Hvidt, W. Brown, and K. Schillén, *Macromolecules*, **30**, 2355 (1977).
(18) M. J. Park and K. Char, *Macromol. Rapid Commun.*, **23**, 688 (2002).
(19) B. Nyström and H. Walderhang, *J. Phys. Chem.*, **100**, 5433 (1996).
(20) A. Kelarakis, V. Castelletto, C. Chaibundit, J. Fundin, V. Havredaki, I. W. Hamley, and C. Booth, *Langmuir*, **17**, 4232 (2001).
(21) I. W. Hamley, in *The Physics of Block Copolymers*, Oxford, 1998.